Journal of Membrane Science and Research 1 (2015) 90-95

Journal of Membrane Science and Research

journal homepage: www.msrjournal.com

Research Paper

Mathematical Modeling of Gas Separation Process with Flat Carbon Membrane

Gohar Gholami[1], Mansooreh Soleimani[1], Maryam Takht Ravanchi[2]

[1] *Department of Chemical Engineering, Amirkabir University of Technology, No.424, Hafez Ave., PO Box 15875-4413, Tehran, Iran*
[2] *Catalyst Research Group, Petrochemical Research and Technology Company, National Petrochemical Company, Tehran, Iran*

HIGHLIGHTS

- Mathematical modeling of gas separation process with carbon membrane.
- Considering flat configuration of carbon membrane.
- Surveying binary diffusion through the membrane.

GRAPHICAL ABSTRACT

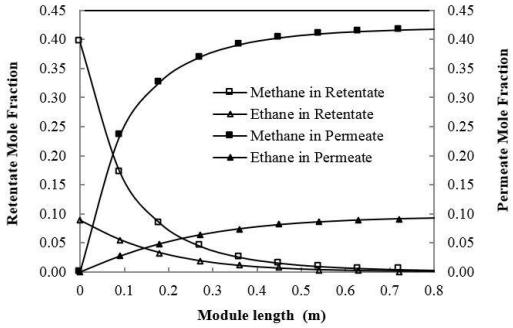

ARTICLE INFO

Article history:
Received 2014-09-03
Revised 2014-11-28
Accepted 2014-12-02
Available online 2014-12-03

Keywords:
Carbon molecular sieve membrane
CMSM
Flat membrane
Gas separation
Modeling

ABSTRACT

Carbon molecular sieve membranes (CMSMs) have been considered as very promising candidates for gas separation, in terms of separation properties as well as thermal and chemical stability. Due to the numerous advantages and wide applications of carbon membranes, their application for gas separation is of special importance. Because of the importance of carbon membranes and a large number of studies in the field of carbon membrane fabrication, in this study, mathematical modeling of the gas separation process in CMSMs has been investigated. Flat configuration is considered for the membrane, which has been applied for the separation process of CH_4 and C_2H_6. The Runge-Kutta method has been applied in order to solve the model. In the mentioned model, the sorption-diffusion mechanism has been considered as a dominant one for gas separation with CMSM. By comparing theoretical results with experimental ones for binary diffusion, good agreement was obtained. Finally, the effect of some parameters such as effective area of the module, module temperature, total feed pressure and feed flow rate on the purity of components in the retentate and permeate stream and recovery of fast components in the permeate stream have been investigated. Results demonstrated that increasing the effective area, membrane temperature and total feed pressure increased the recovery of the fast component in the permeate side, while the feed flow rate had an adverse effect.

1. Introduction

Conventional technologies for gas separation such as distillation, crystallization, absorption, adsorption, solvent extraction, or cryogenics have been optimized for decades [1,2]. In recent decades, higher energy costs, energy intensive methods and adverse impact on the environment have made the membrane processes competitive with other separation technologies. New studies have been focused on inorganic membranes [3] and among them, carbon membranes are promising candidates for gas separation because of their thermal and chemical stability and some unique advantages for many

* Corresponding author at: Tel./fax: +98 (21) 66405847
E-mail address: soleimanim@aut.ac.ir (M. Soleimani)

industrial applications [4-6]. Although the concept of carbon membrane for gas separation dated back to 1970, the interest to develop the carbon membrane grew since Koresh and Soffer [7,8] successfully prepared the crack-free molecular sieve hollow fiber carbon membrane by carbonizing cellulose hollow fiber.

Nowadays, new researchers are trying to prepare a carbon membrane, using different kinds of polymeric materials, which are resulting in different kinds of carbon membranes [9-14] and the different conditions of preparing the carbon membrane [15]. There is a considerable amount of published experimental data on the permeability of pure components through CMSMs [7,16-18], but there is little data on equilibrium adsorption, diffusion coefficient and multi-component transport [7]. Therefore, the large part of researches on the carbon membrane belongs to its preparation process [8,16,18-21]. There have also been reports on supported carbon membranes [22-25], composite carbon membranes [26-28] and mixed matrix membranes. Also, other reports include experimental data of pure component permeability and recently experimental data on adsorption equilibrium, diffusion coefficient [7,16,23] and multi-component transport [20,23,24,28].

According to the mentioned researches, it can be seen that the main portion of the studies have been experimental ones. However, it is noticeable that mathematical modeling also plays an important role in designing new equipment and processing optimization. Therefore, modeling of the gas separation process with carbon membranes in different configurations has great importance. This study has been focused on the modeling of the gas separation process with flat carbon membrane.

2. Model development

2.1. Membrane fundamentals

Mass transfer in the membrane module consists of molecular diffusion (Equation (1)), bulk diffusion (Equation (2)) and permeation through the membrane.

$$J_i\big|_x = -D_i \frac{\partial C_i}{\partial x} \tag{1}$$

$$n_i^0\big|_x = C_i u_i A \tag{2}$$

where D_i,is diffusion coefficient of component i, C_i is molar concentration of component i, u_i velocity of component i and A is the cross section of gas passage in retentate or permeate side of the membrane.

In this modeling, the sorption-diffusion mechanism has been considered as a dominant one for gas separation with CMSM and has been defined from the Langmuir isotherm (Equation (3)):

$$\frac{q_i}{q_{si}} = \frac{b_i p_i^{n_i}}{1 + b p_i^{n_i}} \tag{3}$$

where p_i is partial pressure of component i, q_i is the concentration of component I in the adsorbed phase, q_{si} is its saturation capacity, b_i is the affinity coefficient of component I and n_i is Langmuir constant of component i.

Binary or multicomponent diffusivities through CMSM are strongly concentration dependent and can be calculated by proposed relations of Yang et al. [23] (Equations (4) and (5)):

$$D_{ij} = \frac{D_{i0}[(1-\lambda_{ij})\theta_i]_{j\neq i}}{[1-\sum_{j=1}^{n}(1-\lambda_{ij})\theta_j]} \tag{4}$$

$$D_{ii} = D_{i0}\frac{\left[1-\sum_{j=1}^{n}(1-\lambda_{ij})\theta_j\right]_{j\neq i}}{1-\sum_{j=1}^{n}(1-\lambda_{ij})\theta_j} \tag{5}$$

where D_{i0} is pure component diffusivity at zero coverage of component i,θ_i is surface coverage of component i and λ_{ij} is interaction parameter of component i and j. Component diffusivity at zero coverage can be described as a function of temperature (Equation (6)):

$$D_{i0} = D_{i0}^{*} e^{\frac{-E_a}{RT}} \tag{6}$$

where is pre-exponential factor of component i, E_a is activation energy, R is gas constant and T is module temperature. In addition, λ_{ij} (interaction of component i, sticking on adsorbed molecule j), can be calculated from Equation (7):

$$\lambda_{ij} = e^{-(e_{iv}-e_{ij})/RT} \tag{7}$$

where, e_{iv} is activation energy for diffusion on the bare surface, which can be considered as heat of adsorption and e_{ij} is activation energy for diffusion on adsorbed molecules (Equation (8)).

$$e_{ij} = e_{ji} = (e_{ii}e_{jj})^{1/2} \tag{8}$$

Therefore, for binary diffusion of components, flux can be written as Equation (9).

$$J_{im} = -\frac{1}{\delta}\sum_{j=1}^{2}[\bar{D}_{ij}(q_{jout}-q_{jin})] \tag{9}$$
$$i = A,B$$
$$j = A,B$$

where, δ is the membrane thickness and is the average amount of binary diffusion coefficient, which can be determined from Equation (10):

$$\bar{D}_{ij} = \frac{1}{q_{j_{out}} - q_{j_{in}}}\int_{q_{j_{in}}}^{q_{j_{out}}} D_{ij}(\bar{q}_i, q_j)dq_j \tag{10}$$

where, the subscripts in and out stand for conditions on the two sides of the membrane and $\bar{q}_i$, is the average adsorbed amount of component i and can be obtained as follows:

$$\bar{q}_i = \frac{q_{ir} + q_{ip}}{2} \tag{11}$$

Subscripts r and p refer to retentate and permeate side of the membrane, respectively. For a binary system including components and, q_s can be calculated from Equation (12):

$$\frac{1}{q_{st}} = \frac{X_A}{q_{sA}} + \frac{X_B}{q_{sB}} \tag{12}$$

X_i is the adsorbed phase mole fraction at equilibrium of component i. In addition, surface coverage for component A and B are in the form of Equation (13).

$$\theta_A = \frac{q_A}{q_{st}},\ \theta_B = \frac{q_B}{q_{st}} \text{ and } \theta_A + \theta_B \leq 1 \tag{13}$$

2.2. Assumptions and model equations

A schematic diagram of a flat carbon membrane has been shown in Figure 1. According to this figure, feed enters the membrane module and based on the pressure difference between two sides of the membrane, the species penetrate through the membrane with different velocities. The species that can pass through the membrane are called permeate, while those being rejected by the membrane are called retentate.

Material balances have been carried out on the feed side and permeate side of the membrane module. Figure 2 shows a differential distance in the flat membrane and the mass balance that has been applied in it. It should be noted that in this modeling, the binary gas separation process is the required object.

The applied assumptions have been mentioned below:

1. Membrane layer is lumped.
2. Isothermal condition prevails in the module.
3. Process is steady-state.
4. Gas flow in the membrane module is co-current
5. Velocity in the module is constant.
6. The length of the module is too long in comparison with other directions.
7. y direction of the system is considered solid.
8. Molecular diffusion is negligible in comparison with bulk diffusion in x direction.

9. Ideal gas behavior is considered.
10. Gas is incompressible.
11. Carrier gas does not permeate through the membrane.

Mass balance for component i in the feed side is as follows:

$$\left(J_i|_x A_x - J_i|_{x+\Delta x} A_x\right)+\left(J_i|_y A_y - J_i|_{y+\Delta y} A_y\right)+\left(J_i|_z A_z - J_i|_{z+\Delta z} A_z\right)+\left(n_i^0|_x - n_i^0|_{x+\Delta x}\right) +\left(n_i^0|_y - n_i^0|_{y+\Delta y}\right)+\left(n_i^0|_z - n_i^0|_{z+\Delta z}\right)-d\left(J_{im} A_{eff}\right)=0 \quad (14)$$

By considering the above assumptions and substituting Equations (1), (2) and (9) in Equation (14), Equation (15) will be obtained:

$$\frac{dp_{ir}}{dx} = -\frac{RT}{Q_r} w J_{im} \quad (15)$$

By applying mass balance and considering the mentioned assumption in the permeate side of the membrane, Equation (16) will be obtained:

$$\frac{dp_{ip}}{dx} = \frac{RT}{Q_p} w J_{im} \quad (16)$$

Boundary conditions are as follows:

$$x = 0 \quad \begin{matrix} p_{ir} = p_{if} \\ p_{ip} = p_{is} \end{matrix} \quad (17)$$

In order to obtain the pressure distribution along the membrane module, Equations (15) and (16) must be solved together. It can be seen that the equations obtained from the modeling of the flat carbon membrane are non-linear ordinary differential equations (ODE) and a kind of initial value problem. Thus, in order to solve the equations, the Forth Runge-Kutta method has been applied.

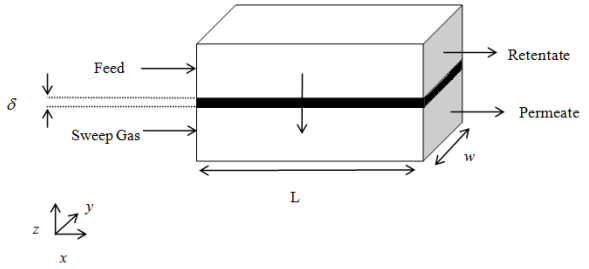

Fig.1. A general scheme of the proposed flat membrane module.

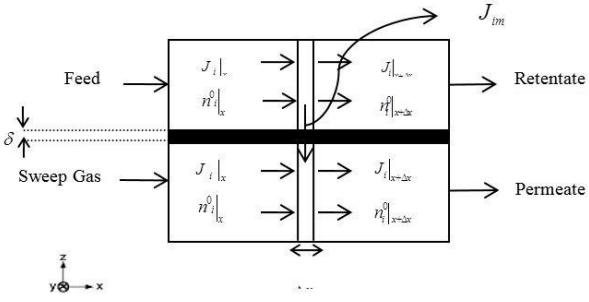

Fig. 2. Mass balance in different distances of the flat membrane.

3. Result and discussion

3.1. Validation of the model

In 1994, Chen and Yang [23] prepared a flat CMSM. They measured steady-state diffusion fluxes of single-component and binary mixtures of CH_4/C_2H_6 through the membrane. Then, in order to verify the validation of their results, they compared the results with the theory of permeation flux. So continuing Chen and Yang's work, in this study, modeling of the membrane module has been done and the obtained results of permeation flux have been compared with the experimental flux of Chen and Yang [23] for two temperatures of 323 K and 353 K. This comparison is reported as the percentage of absolute error in Tables 1 and 2. It should be noted that feed stream includes methane, ethane and Helium as carrier gas, in which case only methane and ethane permeate through the carbon membrane. In turn, it has been called binary diffusion.

Table 1
Binary diffusion of CH_4/C_2H_6 through CMSM at 323 K.

Feed mole fraction		Model flux of binary diffusion (10^{-5} mol.m^{-2}.s^{-1})		Experimental flux of binary diffusion [23] (10^{-5} mol.m^{-2}.s^{-1})		Percentage of absolute error	
CH_4	C_2H_6	CH_4	C_2H_6	CH_4	C_2H_6	CH_4	C_2H_6
0.203	0.117	4.80	1.62	5.63	1.73	14.00	6.00
0.316	0.062	1.20	1.20	1.10	1.23	9.00	2.40
0.395	0.089	12.70	1.28	12.80	1.32	0.78	3.00
0.499	0.088	18.00	1.02	16.40	0.94	9.70	8.80

Table 2
Binary diffusion of CH_4/C_2H_6 through CMSM at 353K.

Feed mole fraction		Model flux of binary diffusion (10^{-5} mol.m^{-2}.s^{-1})		Experimental flux of binary diffusion [23] (10^{-5} mol.m^{-2}.s^{-1})		Percentage of absolute error	
CH_4	C_2H_6	CH_4	C_2H_6	CH_4	C_2H_6	CH_4	C_2H_6
0.221	0.106	6.3	1.8	6.43	1.743	2	3
0.477	0.142	16.0	1.8	14.00	1.990	14	9
0.252	0.395	5.7	6.9	6.56	7.950	13	13

According to the present model, transport characteristics of the carbon membrane have been illustrated in Table 3. In addition, the characteristics of the flat carbon membrane used in the current study have been mentioned in Table 4.

Single-component equilibrium and diffusivity parameters on the carbon molecular sieve, which are mentioned in the Appendix, have been determined according to Chen and Yang [23].

Tables 1 and 2 show that the error between the experimental results and modeling ones are between 0.78 to 14 percent. It can be seen that the lower error is related to the diffusion at 323K with the mentioned mole fractions: methane 0.395, ethane 0.089 and the other portion refers to the carrier gas. Therefore, these conditions have been applied in the following study of the flat carbon membrane.

Table 3
Transport Characteristics

H_4 Permeance ($m^3.m^{-2}.Pa^{-1}.s^{-1}$)	6×10^{-7}
C_2H_6 Permeance ($m^3.m^{-2}.Pa^{-1}.s^{-1}$)	2×10^{-7}
Separation Factor (CH_4/ C_2H_6)	2.73

Table 4
The characteristic of the flat carbon membrane [23].

Effective Area (m^2)	Thickness (m)	Length (m)	Density (kg.m^{-3})
0.3	15×10^{-6}	0.8	2.15×10^{3}

3.2. Mole fraction distributions in the length of the membrane module

To the best of our knowledge, the fast component tends to permeate through the membrane, while the slow one tends to remain in the retentate side. In this binary system, methane is the fast component and ethane is the slow one. So, although Figure 3 shows that mole fraction of the components decrease in the retentate side and increase in the permeate side along the module, the increase of methane in the permeate side is much more than ethane and the increase of ethane in the retentate side is higher. Therefore, as it was expected, the permeate side of the module becomes rich from methane and the retentate side of the module becomes rich from ethane.

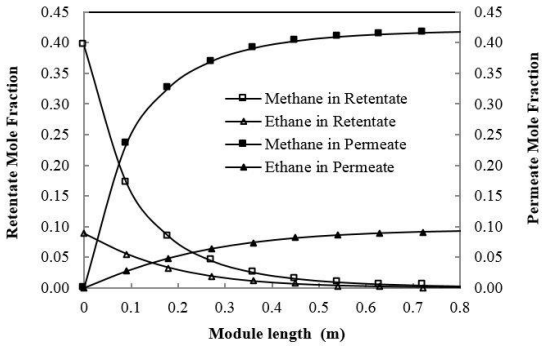

Fig. 3. CH_4 and C_2H_6 mole fraction distribution in the retentate and permeate side, along the length of the module.
(T=323 K, $y_{methane\,f}$=0.395, $y_{ethane\,f}$=0.089, y_{cf}=0.516, P_f=106.7kPa, Q_f=4×10^{-7}, Q_s=2×10^{-5}, L=0.8 m)

3.3. Effect of membrane area on separation performance

Figures 4 and 5 show the effect of the membrane area on the separation performance along the membrane length. Results of modeling suggest that although increasing the effective area of the membrane decreases the mole fraction of both components in the retentate side, the decrease of methane is more than ethane, so the retentate side of the membrane becomes rich from ethane. Similarly, an increase of methane in the permeate side is more than ethane, so the permeate side of the module becomes rich from methane. As it can be seen, increasing the membrane area benefits the separation and increases the methane recovery in the permeate side of the module (Figure 6). According to these figures, it is noticeable that increasing the effective area from 0.15 to 0.25 m2 is more effective than increasing the area from 0.25 to 0.35 m2. This subject is also obvious in the amount of methane recovery in the permeate side. Therefore, it should be noted that the effective area has an optimum point, since after this point it is not affordable.

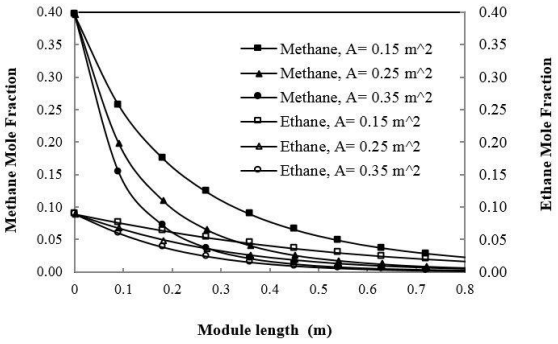

Fig. 4. The effect of membrane area on methane and ethane mole fraction in retentate side, along the module length.
(T=323 K, $y_{methane\,f}$=0.395, $y_{ethane\,f}$=0.089, y_{cf}=0.516, P_f=106.7kPa, Q_f=4×10^{-7}, Q_s=2×10^{-5}, L=0.8 m)

3.4. Effect of feed pressure on separation performance

By increasing the feed pressure, the driving force of permeation through the membrane increases. Thus, it is anticipated that increasing the feed pressure benefits the separation. Figure 7 shows that by increasing the feed pressure, the methane purity in the permeate side and ethane purity in the retentate side increases. Furthermore, in Figure 8 it can be seen that increasing the feed pressure increases the amount of methane recovery in the permeate side of the module. The other observation of Figure 7 is that increasing the feed pressure from 66.7 to 106.7 kPa leads to more ethane purity in the retentate side, in comparison with feed pressure in the range of 40-66.7 kPa. As a result, in the range of 66.7 to 106.7 kPa of feed pressure, better separation has been obtained.

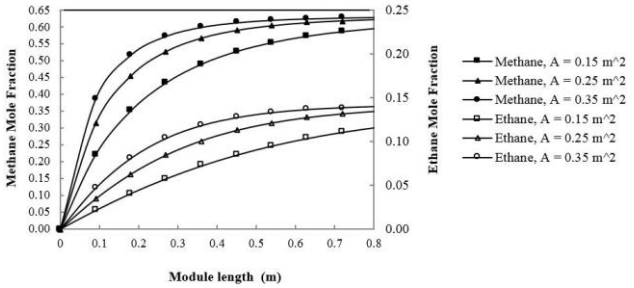

Fig. 5. The effect of membrane area on methane and ethane mole fraction in permeate side along the module length.
(T=323 K, $y_{methane\,f}$=0.395, $y_{ethane\,f}$=0.089, y_{cf}=0.516, P_f=106.7kPa, Q_f=4×10^{-7} , Q_s=2×10^{-5} , L=0.8 m)

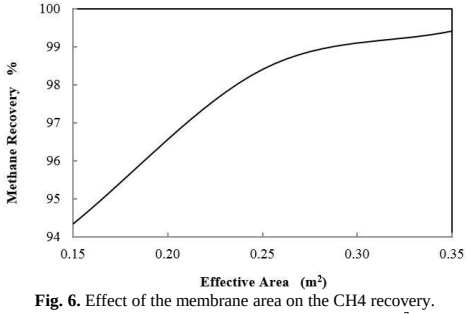

Fig. 6. Effect of the membrane area on the CH4 recovery.
(T=323 K, $y_{methane\,f}$=0.395, $y_{ethane\,f}$=0.089, y_{cf}=0.516, P_f=106.7kPa, Q_f=4×10^{-7}, Q_s=2×10^{-5}, L=0.8 m)

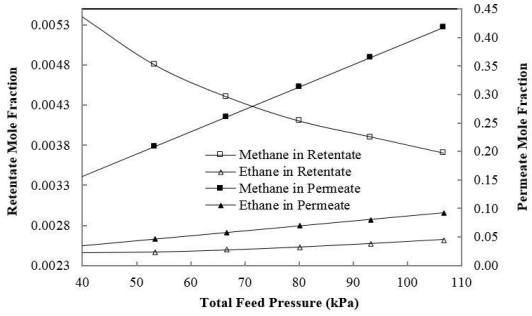

Fig. 7. Effect of feed pressure on mole fraction in the retentate and permeate streams.
(T=323 K, $y_{methane\,f}$=0.395, $y_{ethane\,f}$=0.089, y_{cf}=0.516,A_{eff}=0.3 m^2, Q_f=4×10^{-7} , Q_s=2×10^{-5} , L=0.8 m)

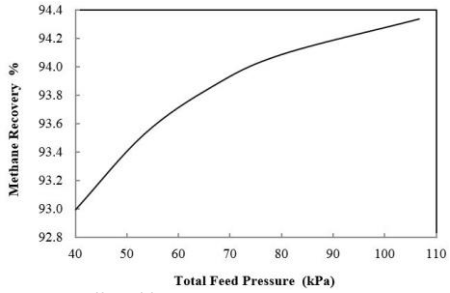

Fig. 8. Effect of feed pressure on the methane recovery.
(T=323 K, $y_{methane\,f}$=0.395, $y_{ethane\,f}$=0.089, y_{cf}=0.516,A_{eff}=0.3 m^2, Q_f=4×10^{-7} , Q_s=2×10^{-5} , L=0.8 m)

3.5. Effect of feed flow rate on separation performance

It is important to bear in mind that the existence of a driving force leads to the separation process. Hence, the more the gas residence time in the module, the more separation will be achieved. Thus, by increasing the feed flow rate, gas velocity increases and retention time decreases. As a result, increasing the feed flow rate does not benefit the separation. As it was expected, Figure 9 shows that increasing the feed flow rate increases the purity of both components in the permeate side, but decreases the amount of methane recovery in the permeate side (Figure 10).

3.6. Effect of temperature on separation performance

By and large, by elevating the temperature, gas adsorption decreases. However, diffusion through the membrane rises, in which case, diffusion of methane is more than ethane (Figure 11), due to its higher interaction parameter and lower diffusion activation energy. The mentioned results can be derived respectively from Equations (6) and (7). This leads to the condition in which the permeation flux of methane and ethane increases; however, the elaboration amount of methane is more than ethane. As a result, the permeate side of the membrane becomes rich from methane and retentate becomes rich from ethane (Figure 11) and recovery of methane burgeons (Figure 12).

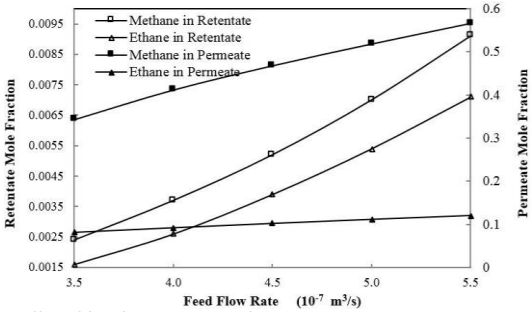

Fig. 9. Effect of feed flow rate on mole fraction in the retentate and permeate streams.
(T=323 K, $y_{methane\,f}$=0.395, $y_{ethane\,f}$=0.089, y_{cf}=0.516, P_f=106.7kPa, A_{eff}=0.3 m^2, Q_s=2×10^{-5}, L=0.8 m)

4. Conclusion

Inorganic carbon membranes are good candidates for the gas separation process due to their high thermal and chemical stability. Therefore, in this study, modeling of the gas separation process with the flat carbon membrane was applied and compared with experimental data. In this modeling, the separation of CH_4/C_2H_6 has been investigated. By comparing the modeling

results with the experimental ones, good agreement was obtained and the amount of error was between 0 -14%.

Furthermore, after investigating some parameters, the following results were obtained:

-Increasing the feed pressure increases the recovery of the fast component and increases its purity in the permeate stream.
-Increasing the feed flow rate decreases the recovery of the fast component and increases its purity in the permeate stream.
-Increasing the effective area of the membrane increases the recovery and purity of the fast component in the permeate stream.
-Increasing the temperature of the module increases the recovery and purity of the fast component in the permeate stream.

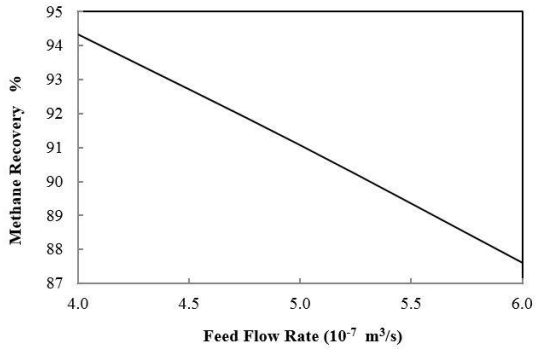

Fig. 10. Effect of feed flow rate on the methane recovery.
(T=323 K, $y_{methane\ f}$=0.395, $y_{ethane\ f}$=0.089, y_{cf}=0.516, P_f=106.7kPa, A_{eff}=0.3 m^2, Q_s=2×10^{-5}, L=0.8 m)

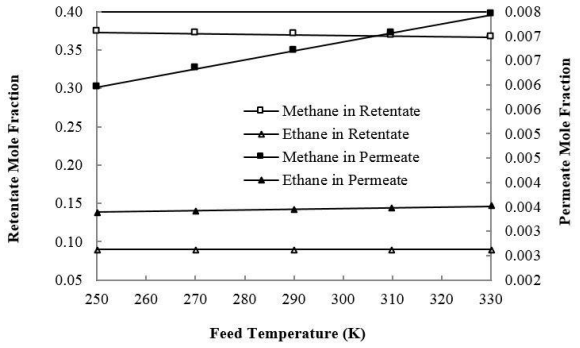

Fig. 11. Effect of feed temperature on mole fraction in the retentate and permeate streams.
($y_{methane\ f}$=0.395, $y_{ethane\ f}$=0.089, y_{cf}=0.516, P_f=106.7kPa, Q_f=4×10^{-7} , Q_s=2×10^{-5} , A_{eff}=0.3 m^2, L=0.8 m)

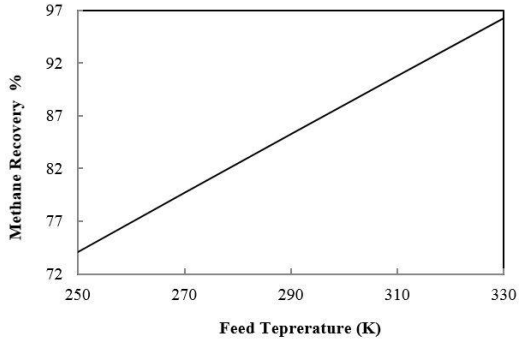

Fig. 12. Effect of feed temperature on the methane recovery.
($y_{methane\ f}$=0.395, $y_{ethane\ f}$=0.089, y_{cf}=0.516, P_f=106.7kPa, Q_f=4×10^{-7} ,Q_s=2×10^{-5} , A_{eff}=0.3 m^2, L=0.8 m)

Nomenclature

A	Cross sectional area *(m^2)*
b_i	Langmuir constant for component *i (bar^{-1})*
C_i	Molar concentration of component *i (mol.m^{-3})*
D_i	Diffusion coefficient of component *i (m^2.s^{-1})*
D_{i0}	Pure component diffusivity at zero coverage of component *i (m^2.s^{-1})*
D_{i0}^*	Pre exponential factor of component *i (m^2.s^{-1})*
D_{ij}	Binary diffusion coefficient *(m^2.s^{-1})*
$\overline{D}_{ij}$	The average amount of binary diffusion coefficient *(m^2.s^{-1})*
E_a	Diffusion activation energy *(J.mol^{-1})*
e_{ij}	Activation energy for diffusion on adsorbed molecules *(J.mol^{-1})*
e_{iv}	Activation energy for diffusion on bare surface *(J.mol^{-1})*
J_i	Diffusion flux of component *i (mol.m^{-2}.s^{-1})*
J_{im}	Permeation flux of component *i* through the membrane *(mol.m^{-2}.s^{-1})*
L	Module length *(m)*
n_i^0	Bulk mass transfer of component *i (mol.s^{-1})*
n_i	Langmuir constant of component *i*
p_i	Partial pressure of component *i (Pa)*
P_f	Total feed pressure *(Pa)*
q_i	Adsorbed amount of component *i (mol.kg^{-1})*
q_{si}	Saturated adsorbed amount of component *i (mol.kg^{-1})*
$\overline{q}_i$	Average adsorbed amount of component *i (mol.kg^{-1})*
Q_j	Volumetric flow rate of stream *j (m^3.s^{-1})*
R	Gas constant *(J.mol^{-1}.K^{-1})*
T	Module temperature *(K)*
u_i	Velocity of component *i (m.s^{-1})*
w	Module width *(m)*
X_i	Adsorbed phase mole fraction at equilibrium of component *i*
y	Mole fraction

Subscript

A, B	component *A, B*
cf	carrier gas in feed stream
eff	effective area of the membrane
f	feed stream
s	sweep gas stream
i,j	components *i* and *j*
if	component *i* in feed stream
in	side of the membrane that is in contact with the retentate stream
ip	component *i* in permeate stream
ir	component *i* in retentate stream
is	component *i* in sweep gas stream
out	side of the membrane that is in contact with the permeate stream
p	permeate stream
r	retentate stream
st	total saturated adsorbed amount
t	total
x, y, z	coordinate axes

Greek symbol

δ	membrane thickness *(m)*
λ_{ij}	interaction parameter
θ_i	surface coverage of component *i*

References

[1] A.F. Ismail, L.I.B. David, Future direction of R&D in carbon membranes for gas separation, Membr Technology (4) (2003) 4-8.
[2] M. Rungta, L. Xu, W.J. Koros, Carbon molecular sieve dense film membranes derived from Matrimid for ethylene/ethane separation, Carbon 50(4) (2012)1488-1502.
[3] S.T. Hwang, Inorganic membranes and membrane reactors, Korean J. Chem. Eng. 18 (6) (2001) 775-787.
[4] H.P. Hsieh, Inorganic membranes for separation and reaction. Alcoa Technical Center, Alcoa Center, PA, USA, 1996.
[5] G. Gholami, M. Soleimani, M. Takht Ravanchi, A Brief Review of Gas Separation Process with Carbon Membranes, Presented in 3rd International Conference on Environmental Research and Technology (2012).
[6] G. Gholami, M. Soleimani, M. Takht Ravanchi, Application of carbon membranes for gas separation: A Review, J. Ind. Res. Technol. 3 (1) (2013) 53-58.
[7] S. Lagorsse, F.D. Magalhaes, A. Mendes, Carbon molecular sieve membranes: Sorption, kinetic and structural characterization, J. Membr. Sci. 241 (2) (2004) 275-287.
[8] C.W. Jones, W.J. Koros, Carbon molecular sieve gas separation membranes-I. Preparation and characterization based on polyimide precursors, Carbon 32 (8) (1994) 1419-1425.
[9] Y.K. Kim, H.B. Park, Y.M. Lee, Gas separation properties of carbon molecular sieve membranes derived from polyimide/polyvinylpyrrolidone blends: effect of the molecular weight of polyvinylpyrrolidone, J. Membr. Sci. 251(1-2) (2005) 159-167.
[10] D. Grainger, M.B. Hägg, Evaluation of cellulose-derived carbon molecular sieve membranes for hydrogen separation from light hydrocarbons, J. Membr.Sci. 306 (1-2) (2007) 307-317.
[11] S.M. Saufi, A.F. Ismail, Fabrication of carbon membranes for gas separation-a review, Carbon 42 (2) (2004) 241-259.
[12] Y.J. Fu, K.S. Liao, C.C. Hu, K.R. Lee, J.Y. Lai, Development and characterization of micropores in carbon molecular sieve membrane for gas separation, Micropor. Mesopor. Mater. 143 (1) (2011) 78-86.
[13] L. Xu, M. Rungta, W.J. Koros, Matrimid derived carbon molecular sieve hollow fiber membranes for ethylene/ethane separation, J. Membr. Sci. 380 (1) (2011) 138-147.

[14] M. Kiyono, P.J. Williams, W.J. Koros, Effect of polymer precursors on carbon molecular sieve structure and separation performance properties, Carbon 48 (15) (2010) 4432-4441.
[15] H.J. Lee, H. Suda, K. Haraya, D.P. Kim, Influence of oxidation temperature on the gas permeation and separation properties in a microporous carbon membrane, Korean J. Chem. Eng. 23 (3) (2006) 435-440.
[16] K. Wang, H. Suda, K. Haraya, The characterization of CO_2 permeation in a CMSM derived from polyimide, Sep. Purif. Technol. 31 (1) (2003) 61-69.
[17] Y.S. Bae, C.H. Lee, Sorption kinetics of eight gases on a carbon molecular sieve at elevated pressure, Carbon 43 (1) (2005) 95-107.
[18] C. Nguyen, D.D. Do, K. Haraya, K. Wang, The structural characterization of carbon molecular sieve membrane (CMSM) via gas adsorption, J. Membr. Sci. 220 (1-2) (2003) 177-182.
[19] N. Tanihara, H. Shimazaki, Y. Hirayama, S. Nakanishi, T. Yoshinaga, Y. Kusuki, Gas permeation properties of asymmetric carbon hollow fiber membranes prepared from asymmetric polyimide hollow fiber, J. Membr. Sci. 160 (2) (1999) 179-186.
[20] D.Q. Vu, W.J. Koros, S.J. Miller, High pressure CO2/CH4 separation using carbon molecular sieve hollow fiber membranes, Ind. Eng. Chem. Res. 41 (3) (2002) 367-380.
[21] T.A. Centeno, A.B. Fuertes, Carbon molecular sieve gas separation membranes based on poly (vinylidene chloride-co-vinyl chloride), Carbon 38 (7) (2000) 1067-1073.
[22] A.B. Fuertes, T.A. Centeno, Preparation of supported carbon molecular sieve membranes, Carbon 37 (4) (1999) 679-684.
[23] Y.D. Chen, R.T. Yang, Preparation of carbon molecular sieve membrane and diffusion of binary mixtures in the membrane, Ind. Eng. Chem. Res. 33 (12) (1994) 3146-3153.
[24] M.G. Sedigh, L. Xu, T.T. Tsotsis, M. Sahimi, Transport and morphological characteristics of polyetherimide-based carbon molecular sieve membranes, Ind. Eng. Chem. Res. 38 (9) (1999) 3367-3380.
[25] T.A. Centeno, A.B. Fuertes, Supported carbon molecular sieve membranes based on a phenolic resin, J. Membr. Sci. 160 (2) (1999) 201-211.
[26] A.B. Fuertes, D.M. Nevskaia, T.A. Centeno, Carbon composite membranes from Matrimid and Kapton polyimides for gas separation, Micropor. Mesopor. Mater. 33 (1-3) (1999) 115-125.
[27] C.W. Jones, W.J. Koros, Carbon composite membranes: a solution to adverse humidity effects, Ind. Eng. Chem. Res. 34 (1) (1995) 164-167.
[28] J.L. Soares, H.J. Jose, R. Moreira, Preparation of a carbon molecular sieve and application to separation of N2, O2 and CO2 in a fixed bed, Brazilian J. Chem. Eng. 20 (1) (2003) 75-80.

Appendix

Table A1
Single-component equilibrium and diffusivity parameters on carbon molecular sieve membrane.

Sorbate	T (K)	q_s ($mol.kg^{-1}$)	b (bar^{-1})	n	λ	$D_{i0}\times10^{12}$ ($m^2.s^{-1}$)
CH_4	297	1.145	0.368	1.24	0.056	1.695
	323	1.051	0.338	1.21	0.195	2.429
	353	0.797	0.316	1.22	0.280	3.438
C_2H_6	297	2.072	15.001	0.84	0	0.146
	323	1.821	3.975	1.03	0	0.188
	353	1.549	3.705	0.99	0	0.315

Table A2
Energetic parameters and pre-exponential factor for diffusivity in carbon molecular sieve membrane.

Sorbate	$E_a\times10^{-3}$ ($J.mol^{-1}$)	$D_{i0}^{*}\times10^{10}$ ($m^2.s^{-1}$)
CH_4	10.502	1.22
C_2H_6	12.426	0.21